Pertanika J. Sci. & Technol. 25 (S): 39 - 48 (2017)

SCIENCE & TECHNOLOGY

Journal homepage: http://www.pertanika.upm.edu.my/

Lumen-Nuclei Ensemble Machine Learning System for Diagnosing Prostate Cancer in Histopathology Images

Dheeb Albashish[1]*, Shahnorbanun Sahran[2], Azizi Abdullah[2], Nordashima Abd Shukor[3] and Suria Hayati Md Pauzi[3]

[1]Computer Science Department, Prince Abdullah Bin Ghazi Faculty of Information Technology, Al-Balqa Applied University, Jordan.
[2]Pattern Recognition Research Group, Center for Artificial Intelligence Technology, Faculty of Information Science and Technology, University Kebangsaan Malaysia, 43600 Bangi, Malaysia
[3]Department of Pathology, University Kebangsaan Malaysia Medical Center, Malaysia

ABSTRACT

The Gleason grading system assists in evaluating the prognosis of men with prostate cancer. Cancers with a higher score are more aggressive and have a worse prognosis. The pathologists observe the tissue components (e.g. lumen, nuclei) of the histopathological image to grade it. The differentiation between Grade 3 and Grade 4 is the most challenging, and receives the most consideration from scholars. However, since the grading is subjective and time-consuming, a reliable computer-aided prostate cancer diagnosing techniques are in high demand. This study proposed an ensemble computer-added system (CAD) consisting of two single classifiers: a) a specialist, trained specifically for texture features of the lumen and the other for nuclei tissue component; b) a fusion method to aggregate the decision of the single classifiers. Experimental results show promising results that the proposed ensemble system (area under the ROC curve (Az) of 88.9% for Grade 3 versus Grad 4 classification task) impressively outperforms the single classifier of nuclei (Az=87.7) and lumen (Az=86.6).

Keywords: Ensemble machine learning, Gleason grading system, Lumen, Nuclei, Prostate cancer histological image, Tissue components

ARTICLE INFO

Article history:
Received: 15 August 2016
Accepted: 18 May 2017

E-mail addresses:
bashish@bau.edu.jo (Dheeb Albashish),
shahnorbanun@ukm.edu.my (Shahnorbanun Sahran),
azizia@ukm.edu.my (Azizi Abdullah),
nordashima@ppukm.ukm.edu.my (Nordashima Abd Shukor),
su_hayati@ppukm.ukm.edu.my (Suria Hayati Md Pauzi)
*Corresponding Author

ISSN: 0128-7680

INTRODUCTION

A common and traditional method for prostate cancer diagnosis is via a microscopic analysis of prostate biopsy tissue samples. Histopathologists analyse the tissue biopsy samples under a microscope, then diagnose and grade the tissue based on the texture of the tissue components (e.g. lumen and

nuclei). The pathologists examine the tissue at a high magnification (e.g., 40x) and utilise the tissue components and their texture features to distinguish benign (normal) from malignant (i.e. cancerous) tissue, and identify the tumour malignancy using the Gleason grade scheme (Gleason, 1977). The Gleason grading scheme consists of five numerical grades starting from least aggressive (Grade 1) to most aggressive (Grade 5). Gleason grade 3 and 4 share many similarities in terms of their textures. Thus, to differentiate between grade 3 versus grade 4 is a challenging task (Mosquera-Lopez, Agaian, Velez-Hoyos, & Thompson, 2014; Nguyen, Sabata, & Jain, 2012).

Manual process of diagnosing prostate cancer and grading has a few drawbacks. For instance, the process is subjective and can lead to biased opinion due to experience and personal skills of the pathologists. It leads to inter- and intra-observer variabilities. Consequently, an accurate computer-added systems (CADs) for prostate cancer diagnosing and grading is desirable.

In most CAD- based diagnosis for prostate cancer, the features are determined based on the tissue-structure, such as shape, size of the tissue components. Additionally, , the features are extracted from the texture of the image, extracted from the region of interest (ROI) such as in (Diamond et al., 2004). However, the texture features of the spatial distribution of the tissue components has a semantic meaning to a pathologist and used in practice to guide the grading estimation (Khurd et al., 2011; Mosquera-Lopez et al., 2014). Thus, the aim of this paper is to utilise the nuclei and lumen tissue components by extracting the texture features from their spatial distribution within the tissue image to distinguish between Grade 3 versus Grade 4 in prostate cancer (Sparks & Madabhushi, 2013). In addition, Ensemble machine learning is built by fusing the posterior probabilities of the lumen and nuclei classifiers to enhance their performance.

The remainder of this paper is organised as follows: Section 2 discusses major studies and findings on this topic while Section 3 examines the proposed ensemble framework. In section 4, the results of the study are discussed while section 5 concludes the paper. The methods to grade prostate cancer can be categorised as texture-based and structure-based (Mosquera et al., 2014). In the texture based approach, different types of texture features in the histopathology image are employed for tissue classification. Diamond et al., (2004) employed co-occurrence texture features to classify the tissue image into either stroma or prostatic carcinoma. DiFranco, O'Hurley, Kay, Watson, and Cunningham (2011) used the co-occurrence texture features for each colour channel independently to discriminate the textural discrepancy between normal and malignant cells.

In the structure-based approaches, the features are extracted either from specific tissue components (e.g. nuclei) (Doyle, Feldman, Shih, Tomaszewski, & Madabhushi., 2012; Khurd et al., 2011) or the gland structure (Nguyen, Sabata, & Jain, 2012). In (Nguyen, Sabata, & Jain, 2012), Nguyen proposed a method to extract the gland structure features based on the size of lumen and nuclei. However, this method is not successful in differentiating between grades 3 versus 4. In (Nguyen, Sarkar, & Jain, 2012) the authors performed k-means in the RGB space to extract four tissue components, then extract the structure and contextual features from nuclei and lumen. These showed 79% accuracy when evaluated for normal v. cancer classification on

48 images. However, the structure features of the glands fail to detect glands without lumen or glands with multiple lumina (Nguyen, Sarkar, & Jain, 2014).

Most of the studies above used generic texture features to classify a tissue pattern as being or malignant. The texture features of the spatial tissue components were not effectively analysed. In addition to low-level image features, we believe the domain knowledge about texture features of the special distribution of individual tissue components especially nuclei and lumina objects should be used in the classifiers to improve the sensitivity and selectivity of the classification. Therefore, this paper classifies a tissue image as Grade 3 or Grade 4 by building two independent single classifiers models based on textural features of the spatial distribution of nuclei and lumina objects respectively. Later, an ensemble of learning system is built consisting of two single classifiers, where each classifier is trained specifically for one tissue component. Thus, the final grading (Grade 3 versus Grade 4) is done by a combination of method. One of the most popular combination methods is the product rule (Polikar, 2006), which utilise the diversity of classifiers.

MATERIALS AND METHODS

The proposed ensemble lumen-nuclei prostate classification system has five main stages, namely (1) lumen-nuclei tissue component identification, (2) feature extraction, (3) feature selection, (4) training and testing data formulation, and finally, (5) classification of images into Grade 3 or Grade 4 by using an ensemble classifier. Figure 1 presents the top-level architecture of the proposed system. The following subsections describe the details of each stage in the proposed system.

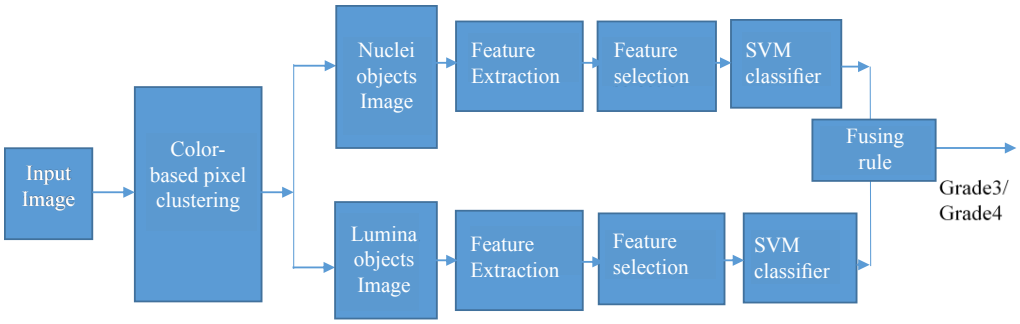

Figure 1. The proposed ensemble lumen-nuclei machine learning system

Lumen-Nuclei Tissue Component Identification

Lumen and nuclei are the most important components of the histopathological image (Nguyen, Sabata, & Jain, 2012). To find the lumina and nuclei objects from the image, K-mean clustering algorithm is applied, where the image pixels (each with RGB components) are partitioned into four clusters (thus, k=4). Each pixel in the image is assigned a label corresponding to one of the four tissue components (lumen, stroma, nuclei, and cytoplasm) (Nguyen, Sarkar, & Jain, 2012). Then, the nuclei and lumen tissue components are extracted as shown in Figure 2.

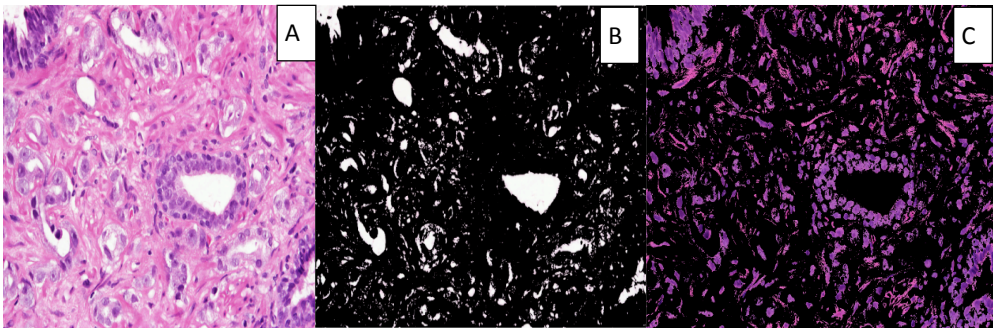

Figure 2. A) Prostate Grade3 H&E histological image, B) The lumen tissue component, and C) The Nuclei Tissue Component

Feature Extraction

Three types of features, namely Haralick (Haralick & Shapiro, 1992), Histogram of Oriented Gradient (HOG) (Dalal & Triggs, 2005) and run-length matrix (Galloway, 1975), have been extracted from nuclei and lumen images individually. A set of variant Haralick features was extracted from two colour models i.e. CIELa*b* and HSV. A set 21 Haralick features was separately computed from each colour channel. Each Haralick feature is extracted from co-occurrence matrixes based on a particular scalar distance (d=1) and four orientations 0, 45, 90, and 135. The following 21 co-occurrence texture feature are computed: entropy, energy, dissimilarity, contrast, inverse difference, correlation, homogeneity, autocorrelation, cluster shade, cluster prominence, maximum probability, sum of squares, sum average, sum variance, sum entropy, difference variance, difference entropy, information measures of correlation-, information measures of correlation -, maximal correlation coefficient, and inverse difference normalised (INN) (Haralick & Shapiro 1992). Thus, 105 Haralick texture features were extracted from each image.

The second type is the HOG features (Dalal & Triggs, 2005), which provide discriminative and robust edge-based information by using the distribution of gradient directions. The HOG texture features are used to exploit the sharp and well-defined edges present in nuclei and lumen images of prostate cancer. In computing HOG features, the nuclei and lumen image are converted into a gray level before the HOG features are extracted from the gray images based on three factors: (a) number of vertical portions of the image, (b) a number of horizontal portions of the image, (c) bin size.

The third type is the run-length matrix (RLMs) which measures the coarseness of texture in a specific direction (Galloway, 1975; Mosquera-Lopez et al., 2014). The RLMs are generated for each segmented image (nuclei or lumen) using different directions (0 ,45 ,90 and 135), then 11 statistical features are derived like in (Al-Kadi, 2010; Tang, 1998). The following 11 RLMs statistical texture features are computed: Short Run Emphasis, Long Run Emphasis, Gray-Level Nonuniformity, Run Length Nonuniformity, Run Percentage, Low Gray-Level Run Emphasis, High Gray-Level Run Emphasis, Short Run Low Gray-Level Emphasis, Short Run High Gray-Level Emphasis, Long Run Low Gray-Level Emphasis, Long Run High Gray-

Level Emphasis (Tang, 1998). The generalised feature vectors for lumen and nuclei are given by Equation 1 and 2 respectively:

$$L_{f=}\{a_{ht}, b_{ht,} H_{ht}, S_{ht}, V_{ht}, Hog_l, Rml_l\} \quad (1)$$

$$N_{f=}\{a_{ht}, b_{ht,} H_{ht}, S_{ht}, V_{ht}, Hog_n, Rml_n\} \quad (2)$$

where L_f , N_f represent the respective features vectors of lumen image, and nuclei image respectively, a_{ht}, b_{ht}, H_{ht}, S_{ht}, V_{ht} are the Haralick features for the a*,b*,H, S, and V channels respectively, Hog_l and Hog_n represent the Hog features of lumen and nuclei images respectively, Rml_l and Rml_n represent the RML of lumen and nuclei images respectively. A total of 197 features were extracted from separated nuclei or lumen images.

Feature Selection. In prostate cancer classification problem, although each segmented image is represented by a set of texture features that tend to characterise the texture from a different perspective, high dimensionality of training dataset results in the problem of "curse of dimensionality" (Mosquera-Lopez et al., 2014; Saeys, Inza, & Larrañaga, 2007). Thus, feature selection technique is performed to reduce the high dimensionality features space by selecting the most discriminative features. It is based on three main approaches: filter, wrapper and embedded. In general, embedded approach presents significant advantages on feature and classifier interaction (Saeys, Inza, & Larrañaga, 2007).

Among the embedded methods, support vector machine- recursive feature elimination (SVM-RFE) (Guyon, Weston, Barnhill, & Vapnik, 2002) are more robust to data over-fitting than other feature selection methods and has shown its efficacy in many fields. Therefore, this study proposes SVM-RFE for selecting the most important features from both nuclei and lumen features.

SVM Classifier. A Support Vector Machine (SVM) is a binary learning algorithm proposed by Vapnik (Cortes & Vapnik, 1995), which is used to analyse and recognise patterns. In this study, two SVM classifiers are employed to learn from the above-selected features to diagnosis the prostate histopathology image and discriminate between Grade 3 versus Grade 4. The first classifier learned using the training features of nuclei images, while the second learnt by using the selected training features of lumen images.

For SVM, Radial- Basis-Function (RBF) kernel was used in the experiment. Initially, the selected features in the training and testing sets were normalised to the interval [-1, +1] to find the SVM parameters C and γ that perform best for the selected features. In order to optimise the classification performance, the parameters were determined using the libsvm (Chang & Lin, 2011) grid-search algorithm. We tried the following values {2-20, ..., 21…, 220} for C and γ respectively. The values which gave the best accuracy performance with threefold cross-validation are picked and used to train on the training set.

Ensemble Method for Combining Classifiers of Nuclei and Lumen. In machine learning, ensemble classifier is becoming increasingly important as they have repeatedly displayed the ability to improve the performance of a single classifier in theory and practice (Chawla & Sylvester, 2007). The ensemble classifier consists of a set of independent trained base classifiers whose predictions are fused to classify new samples. The outputs of all these base classifiers are fused to create an ensemble final output based on a fusion rule. The fusion rules are categorised as (i) a fusion rule that applies to class label, and (ii) class-specific continuous outputs (Polikar, 2006). For example, majority voting is classified as the first group (i). In comparing different fusing rules for ensemble learning, majority voting is as effective as other complicated rule. However, it is not as good as other techniques with the problem of binary classes (Chen, Zhao, & Lin, 2014). Thus, this study utilises the continuous output because it looks to solve the two-class classification problems. Among the continuous output fusion rules, the product rule is the most efficient and simple rule for combining the output of the base classifiers, which is fast and uses all the information available in the outputs of the base classifiers (Abdullah, Veltkamp, & Wiering, 2009). Moreover, the product rule is utilised when the base classifiers operate in independent feature spaces and have small errors. Thus, in this study, the product rule is employed to fuse the output of the lumen and nuclei base classifiers to produce the final decision of the ensemble. In product rule (Eq. 3), the posterior probability outputs $P_j^t(I)$ for class j of t different classifiers (nuclei and lumen) are fused based on the following formula:

$$P(I) = max_{j=1}^{C=2} \prod_{t=1}^{T=2} P_j^t(I) \quad (3)$$

Then, the class with the maximum probability product is considered as the final class label belonging to the test tissue image (I).

RESULTS AND DISCUSSION

Dataset

The dataset consists of a total 149 Haematoxylin and Eosin (H&E)-stained prostate images with 4140 X 3096 pixels. There are 41 images of Grade 3 and 56 of Grade 4, and 52 are benign. The images digitised at 40x optical magnification. Each region of interest was previously extracted from homogeneous patches of whole tissue slides, and experienced pathologists graded it. The average classification performance over 50 different runs for the best parameters are reported, in each run, the dataset is randomly divided into 50% for training and 50% for testing.

Performance Measures

The proposed Ensemble learning system was quantitatively evaluated using widely known performance criteria such as averaged area under ROC curves (Az), accuracy, specificity and sensitivity. The Az and accuracy were used to measure the ensemble performance using the product rule (Eq. 3). Specificity measures how well the ensemble can make a grade 3 identification. Sensitivity measures how reliable the ensemble system is diagnosing Grade 4. All of these criteria are multiplied by 100%.

The performance and significance level of using single nuclei, lumen classifiers and their ensemble for prostate cancer grading (Grade 3 vs. Grade 4) are shown in Table1. The results in Tables 1, 2 and 3 show the impact of the texture features of nuclei and lumen objects in diagnosing and grading the prostate cancer accurately. The hybrid of HOG, RML and Haralick texture were developed by simple concatenation of individual feature set. The hybrid features set have been reduced using SVM-RFE as discussed in section 3.3.

Prostate tissue images have been classified into Grade 3 and Grade 4 classes based on reduced hybrid feature sets. As shown in Table 1, the results demonstrate that the single nuclei classifier achieves up to Az= 87.75±4.8 while Az=86.62±4.2 for the lumen classifier. However, the sensitivity of the lumen classifier (90.5%) was better than the nuclei classifier (89.78). This indicates that the lumen tissue component in the histopathology images is an asset in identifying Grade 4.

In addition, there was a significant difference between nuclei, lumen and their ensemble (p-value=0.0088) in Grade 3 versus Grade 4 (Table 1). The Az value of ensemble was higher than the base classifiers (either nuclei or lumen). Hence, the proposed ensemble is significantly helpful to improve the grading performance. Moreover, it can be seen from Table 1 that the proposed ensemble of nuclei and lumen outperforms the single nuclei and lumen in term of Az, accuracy, sensitivity and specificity. The value of Az significantly increased with about 2.3% and 1.15%, in the order of lumen and nuclei respectively.

Table 1
Performance and statistical significance of the proposed ensemble system for Grade 3 versus Grade 4, averaged over 50 simulation runs

G3 vs. G4	Lumen classifier	Nuclei classifier	Proposed Ensemble	Significant of Ensemble	
				With Lumen	With Nuclei
Az	86.62 ±4.2	87.75±4.8	88.9 ±4.4	0.0088 P<0.01	0.19
Accuracy	87.29±6.29	88.07±4.25	89.5 ± 3.9	0.028 P<0.05	0.06
Sensitivity	90.5±6.3	89.78±5.9	92.7 ± 5.2	0.05 P<0.05	0.006 p<0.01
Specificity	82.1±10.25	85.72±11.02	85.0±10.0	0.1511	….

Table 2
Performance and statistical significance of the proposed ensemble system for benign versus Grade 4, averaged over 50 simulation runss

B vs. G4	Lumen classifier	Nuclei classifier	Proposed Ensemble	Significant of Ensemble	
				With Lumen	With Nuclei
Az	89.2±5.0	90.03±4.43	92.4 ± 4.7	0.0014	0.0107
Accuracy	89.2+ 5.0	89.88±4.5	92.4 ± 4.6	0.0014	0.0057
Sensitivity	90.92±7.5	86.2±7.9	91.07± 7.0	0.9070	0.0011
Specificity	87.53±9.0	93.8±5.5	93.8 ± 7.5	0.0002	…

For benign versus Grade 4 case in prostate cancer diagnosis, the comparison of average classification accuracy (Az) value for the proposed ensemble learning and an individual classifier of nuclei and lumen is listed in Table 2. As shown in Table 2, the proposed Ensemble significantly (p-value=0.0107) outperformed the nuclei and lumen single classifiers. In benign versus Grade 4, the nuclei tissue components fared better than nuclei.

In the case of benign versus Grade 3 (Table 3), the results indicated the proposed ensemble learning and the lumen classifier showed a greater accuracy (Az= 97.0%). However, the nuclei classifier achieved less accuracy around Az=96.0% since the coarse of nuclei images in grade 3 and benign are relatively close to each other (Nguyen, Sabata, & Jain, 2012). Therefore, the nuclei texture features are not suitable for diagnosing benign versus grade 3.

Table 3
Performance and statistical significance of the proposed system for benign versus Grade 3, averaged over 50 simulation runs and statistical significance.

B vs G3	Lumen classifier	Nuclei classifier	Proposed Ensemble	Significant of Ensemble	
				With Lumen	With Nuclei
Az	97.7±2.3	96.0±2.5	97.85±1.9	…	0.0001 p<0.001
Accuracy	97.8±2.1	96.26±2.47	97.9±1.7	…	0.0001 p<0.001
Sensitivity	96.1±4.5	94.5±4.4	97.0±3.64	…	0.0025 p<0.01
Specificity	99.2±1.7	97.6±2.8	98.6±1.84	…	…

Experimental results in Tables 1 to 3 indicate that the proposed ensemble system which combines the posterior probabilities of the nuclei and lumen classifiers can provide significant performance for solving two-class classification tasks in prostate cancer diagnosing and grading. This study also found that the texture features that were extracted from the spatial distribution of nuclei and lumen tissue components can be successfully used for diagnosis and grading prostate cancer, especially Grade 3 versus Grade 4.

In addition, the experiments found the texture features of nuclei instances (tissue component images) are suitable for Grade 3 versus Grade 4, and benign versus Grade 4 cases. This is due to their superior performance over the texture features of lumen images, and the coarseness of nuclei images are higher in Grade 4 than Grade 3, and benign.

CONCLUSION

In this paper, a new ensemble CAD system is proposed for classifying and grading histopathology images of prostate needle biopsies. In this ensemble, two weak classifiers were constructed based on the texture features (Haralick, HOG and RML) of nuclei and lumen tissue components. This was followed by an ensemble learning system which fuses the decision of the nuclei and lumen classifiers using the product rule.

Results have indicated a significant improvement in the classification accuracy by using our ensemble learning comparing single nuclei or lumen classifiers especially when distinguishing between Grade 3 versus Grade 4, the most challenging case in Gleason grade of prostate cancer. A key characteristic of the proposed ensemble CAD is that diverse classifiers were fused in the

ensemble, thus, producing an overall increase in the classification performance. In contrast, to the single classifier, only the texture features of one type of prostate tissue component was used. This ensemble is generic and can be used for the diagnosis of other diseases such as lung and breast cancer by utilising the nuclei and lumen tissue components.

ACKNOWLEDGEMENT

The authors would like to thank Faculty of Information Science and Technology, Universiti Kebangsaan Malaysia, for providing facilities and Financial Support under Fundamental Research Grant Scheme No. DIP-2015-023 entitled "Object Descriptor via Optimized Unsupervised Learning Approaches" and TT-2017-003.

REFERENCES

Abdullah, A., Veltkamp, R. C., & Wiering, M. a. (2009). An ensemble of deep support vector machines for image categorization. *2009 International Conference of Soft Computing and Pattern Recognition, 1*, 301–306.

Al-Kadi, O. S. (2010). Texture measures combination for improved meningioma classification of histopathological images. *Pattern Recognition, 43*(6), 2043–2053.

Chang, C. & Lin, C. (2011). LIBSVM: A library for support vector machines. *ACMTransactions on Intelligent Systems and Technology, 2*(27), 27:1–27.

Chawla, N. V, & Sylvester, J. (2007). Exploiting diversity in ensembles: Improving the performance on unbalanced datasets. *Multiple Classifier Systems, 4472*, 397–406.

Chen, Y., Zhao, X., & Lin, Z. (2014). Optimizing subspace SVM ensemble for hyperspectral imagery classification. *IEEE Journal of Selected Topics in Applied Earth Observations and Remote Sensing, 7*(4), 1295–1305.

Cortes, C., & Vapnik, V. (1995). Support-vector networks. *Machine Learning, 297*(20), 273–297.

Dalal, N., & Triggs, B. (2005). Histograms of oriented gradients for human detection. *Proceedings - 2005 IEEE Computer Society Conference on Computer Vision and Pattern Recognition, CVPR 2005, I*, 886–893.

Diamond, J., Anderson, N., Bartels, P., Peter H., Montironi, Rodolfo, & Hamilton, P. W. (2004). The use of morphological characteristics and texture analysis in the identification of tissue composition in prostatic neoplasia. *Human Pathology, 35*(9), 1121–1131.

DiFranco, M. D., O'Hurley, G., Kay, E. W., Watson, R. W. G., & Cunningham, P. (2011). Ensemble based system for whole-slide prostate cancer probability mapping using color texture features. *Computerized Medical Imaging and Graphics: The Official Journal of the Computerized Medical Imaging Society, 35*(7-8), 629–45.

Doyle, S., Feldman, M., Shih, N., Tomaszewski, J., & Madabhushi, A. (2012). Cascaded discrimination of normal, abnormal, and confounder classes in histopathology: Gleason grading of prostate cancer. *BMC Bioinformatics, 13*(1), 282.

Galloway, M. M. (1975). Texture analysis using gray level run lengths. *Computer Graphics and Image Processing, 4*(2), 172–179.

Gleason, D. F. (1977). Histologic grading and clinical staging of prostatic carcinom. *Urologic Pathology: The Prostate , M. Tannenbaum, Ed. Philadelphia, PA: Lea and Febiger*, 171–197.

Guyon, I., Weston, J., Barnhill, S., & Vapnik, V. (2002). Gene selection for cancer classification using support vector machines. *Machine Learning, 46*, 389–422.

Haralick, R. M., & Shapiro, L. G. (1992). *Computer and robot vision.* Addison-Wesley.

Khurd, P., Grady, L., Kamen, A., Gibbs-Strauss, S., Genega, E. M., & Frangioni, J. V. (2011). Network cycle features: Application to computer-aided Gleason grading of prostate cancer histopathological images. In *Proceedings - International Symposium on Biomedical Imaging* (pp. 1632–1636).

Mosquera, C., Agaian, S., Velez, A., & Thompson, I. (2014). Computer-aided prostate cancer diagnosis from digitized histopathology: A review on texture-based systems. *IEEE Reviews in Biomedical Engineering, PP*(99), 1,1.

Nguyen, K., Sabata, B., & Jain, A. K. (2012). Prostate cancer grading: Gland segmentation and structural features. *Pattern Recognition Letters, 33*(7), 951–961.

Nguyen, K., Sarkar, A., & Jain, A. (2014). Prostate cancer grading: Use of graph cut and spatial arrangement of nuclei. *IEEE Transactions on Medical Imaging, 33*(12), 2254–2270.

Nguyen, K., Sarkar, A., & Jain, A. K. (2012). Structure and context in prostatic gland segmentation and classification. *Medical Image Computing and Computer-Assisted Intervention - MICCAI 2012, 7510*, 115–123. Retrieved from http://link.springer.com/chapter/10.1007/978-3-642-33415-3_15

Polikar, R. (2006). Ensemble based systems in decision making. *IEEE CIRCUITS AND SYSTEMS MAGAZINE, 6*(3), 21–45.

Saeys, Y., Inza, I., & Larrañaga, P. (2007). A review of feature selection techniques in bioinformatics. *Bioinformatics (Oxford, England), 23*(19), 2507–17.

Sparks, R., & Madabhushi, A. (2013). Statistical shape model for manifold regularization: Gleason grading of prostate histology. *Computer Vision and Image Understanding: CVIU, 117*(9), 1138–1146.

Tang, X. (1998). Texture information in run-length matrices - Image processing, IEEE transactions on - IP00_Texture.pdf, 7(11), 1602–1609. Retrieved from http://mmlab.ie.cuhk.edu.hk/archive/2000/IP00_Texture.pdf